Journal of Sound and Vibration (2003) **259**(1), 209–218
doi:10.1006/jsvi.2002.5074, available online at http://www.idealibrary.com on IDEAL®

SOUND ABSORPTION CHARACTERISTICS OF AIR-GAP SYSTEMS IN ENCLOSED CAVITIES

S. W. Kang

Department of Mechanical Systems Engineering, Hansung University, 389, 2-*ga, Samsun-dong, Sungbuk-gu, Seoul* 136-792*, South Korea. E-mail: swkang@hansung.ac.kr*

AND

J. M. Lee

School of Mechanical and Aerospace Engineering , Seoul National University, San 56-1 Shinlim-dong, Kwanak-gu, Seoul 151-742, South Korea

(*Received* 23 *July* 2001)

1. INTRODUCTION

In most researches on Helmholtz resonators [1–8], the main flow of works has focused on effective sound absorption in a pipe or duct by means of more accurate prediction of their resonant frequencies. It may be said that these sound absorbers may not be efficient when it is shaped for suppressing a cavity resonance at a particular frequency identical to one of the resonance frequencies of an enclosed acoustic cavity. The reason may be that the opening of the absorber perforated through a boundary surface surrounding the cavity is relatively too small, compared with the dimensions of the boundary surface. For this reason, most standing waves produced due to cavity resonance are reflected from the boundary surface without being absorbed into the opening. In order to overcome the shortcomings described above, the paper introduces a new type of sound absorber effective in suppressing the cavity resonance of enclosed cavities, especially in low frequencies. The sound absorber is composed by installing a flexible sheet with a thin space below one of the boundary surfaces of a cavity. In the paper, the thin space is called the *air gap*, the flexible sheet is called the *partition sheet* in that the main cavity and the air gap are divided by the sheet, and the sound absorber is named the *air-gap system*. The air-gap system has resonance frequencies at which acoustic resonance energy in the main cavity is absorbed into the air gap. It should be noted in this paper that a resonance frequency equation is obtained in a closed-form equation, which is a function of the thickness of the gap and the surface density of the partition sheet. Furthermore, experiments show that the resonance frequency equation is a useful guide in determining the gap thickness to suppress the resonance of a target acoustic mode, of which the natural frequency is called the *target frequency* in the paper.

2. RESONANCE FREQUENCIES OF THE AIR-GAP SYSTEM

Suppose that two partition sheets are installed below the upper boundary surface as shown in Figure 1(a). It may be imagined that the second partition sheet plays an

0022-460X/02/$35.00

important role when a sound generator in the main cavity is being excited with a harmonic excitation frequency f. Especially, when the excitation frequency coincides with the natural frequency of the vertical acoustic mode with a nodal surface normal to the vertical direction of the cavity, the resonance of the vertical mode may be controlled by changing the input acoustic impedance on the lower side of the second partition sheet. In order to investigate the validity of this idea and simulate the complex air-gap system, the simple one-dimensional model shown in Figure 1(b) is used.

2.1. CLOSE FORM OF RESONANT FREQUENCIES

The resonance frequency equation of the double-gap system can be obtained by letting the imaginary part of the input acoustic impedance on the lower side of mass m_2 be equal to zero as follows [9]:

$$T_1 T_2 \bar{X}_1 \bar{X}_2 - T_1 \bar{X}_1 + T(T_1 T_2 - 1)\bar{X}_2 + 1 - T_1 T_2 = 0. \tag{1}$$

In equation (1), $T = \tan \pi\Omega\eta$, $T_1 = \tan \pi\Omega\eta_1$ and $T_2 = \tan \pi\Omega\eta_2$ are expressed in terms of the dimensionless frequency $\Omega = f_{reso}/f_{c1}$, where f_{reso} denotes the resonance frequency of the air-gap system and f_{c_1} denotes the natural frequency of the fundamental vertical acoustic mode explained in Figure 1(a); the gap ratios $\eta = \Delta L/L$, $\eta_1 = \Delta L_1/L$ and $\eta_2 = \Delta L_2/L$, where L denotes the effective length calculated from the relationship $f_{c_1} = c/(2L)$ when f_{c_1} may be obtained from an acoustic experiment; $\bar{X}_i = \pi\mu_i(\Omega^2 - \Omega_i^2)/\Omega$ is the

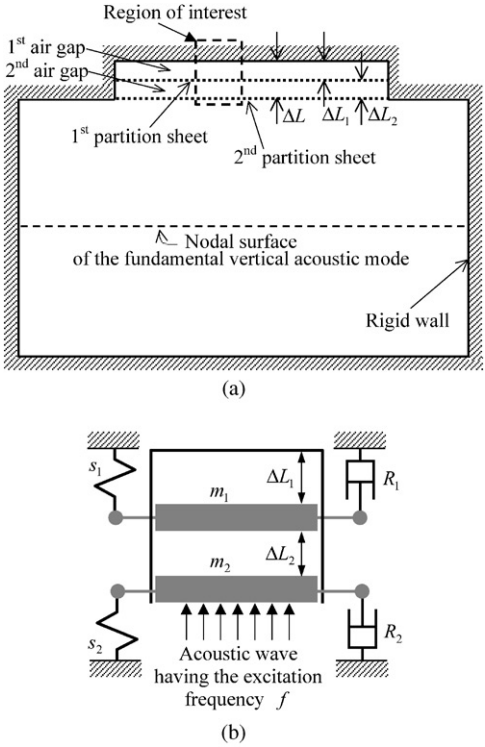

Figure 1. Acoustic cavity with the air-gap system and its theoretical model. (a) double-gap system installed on the upper boundary surface of an enclosed cavity; (b) theoretical model designed from *the region of interest* indicated in (a).

dimensionless form of the imaginary part of the mechanical impedance of m_1 or m_2; $\mu_i = m_i/(\rho LS)$, where ρ is the density of air and S is the area of a contact surface between a main cavity and an air-gap system, represents the mass ratio (this parameter is associated with the surface density of the partition sheet), and $\Omega_i = f_i^{(m)}/f_{c_1}$ denotes the dimensionless natural frequency non-dimensionalized with the fundamental vertical natural frequency f_{c_1} ($f_i^{(m)} = (1/2\pi)\sqrt{s_i/m_i}$ is the natural frequency of m_1 or m_2).

Although the frequency equation, equation (1), may be numerically solved to obtain the resonant frequencies of the air-gap system, this does not give enough information to demonstrate the relationship between the resonant frequencies and the parameters associated with the air-gap system. Thus, a closed- form frequency equation is extracted by applying the long-wavelength limitation [10] to equation (1) under the special condition that the two partition sheets used are identical in material properties: i.e., $\mu_1 = \mu_2 \equiv \mu_s$ and $\Omega_1 = \Omega_2 \equiv \Omega_s$. If partition sheets with the same properties are used, a common mechanical impedance $\bar{X}_s = \pi\mu_s(\Omega^2 - \Omega_s^2)/\Omega = \bar{X}_1 = \bar{X}_2$ can be used instead of $\bar{X}_1$ and $\bar{X}_2$. Using $\bar{X}_s$, equation (1) leads to

$$T_1 T_2 \bar{X}_s^2 + (TT_1 T_2 - T - T_1)\bar{X}_s + 1 - T_1 T_2 = 0, \tag{2}$$

which is explicitly a quadratic equation for $\bar{X}_s$ and the roots of the equation are given by

$$\bar{X}_s = (T + T_1 - TT_1 T_2 \pm \sqrt{D})/(2T_1 T_2), \tag{3}$$

where $D = (TT_1 T_2 - T - T_1)^2 - 4T_1 T_2(1 - T_1 T_2)$. In the current step, an approximation must be considered for D so that a closed-form frequency equation is extracted from equation (3): i.e., terms having orders above $O(T^4)$ vanish after D is fully expanded. This approximation may be valid, because $T = \tan \pi\Omega\eta$, $T_1 = \tan \pi\Omega\eta_1$, and $T_2 = \tan \pi\Omega\eta_2$ have extremely small values thanks to $\eta = \Delta L/L \ll 1$, $\eta_1 = \Delta L_1/L \ll 1$ and $\eta_2 = \Delta L_2/L \ll 1$. Then, equation (3) can be written as

$$\bar{X}_s = (T + T_1 - TT_1 T_2 \pm \sqrt{(T + T_1)^2 - 4T_1 T_2})/(2T_1 T_2) \tag{4}$$

If the *long-wavelength limit* is applied to equation (4): i.e. $T = \tan \pi\Omega\eta \approx \pi\Omega\eta$, $T_1 \approx \pi\Omega\eta_1$, and $T_2 \approx \pi\Omega\eta_2$, and if η_2 vanishes by using $\eta_2 = \eta - \eta_1$ obtained from $\Delta L = \Delta L_1 + \Delta L_2$, equation (4) leads to

$$\bar{X}_s = G/(\pi\Omega\eta), \tag{5}$$

$$G = \left(1 + \gamma \pm \sqrt{5\gamma^2 - 2\gamma + 1}\right)/(2\gamma(1 - \gamma)) = G^{(1)} \text{ or } G^{(2)}, \tag{6}$$

where $\gamma = \eta_1/\eta$ (or $\gamma = \Delta L_1/\Delta L$) represents the proportion of the upper gap thickness to the total gap thickness. Finally, substituting $\bar{X}_s = \pi\mu_s(\Omega^2 - \Omega_s^2)/\Omega$ into equation (5) yields the two resonant frequencies of the double-gap system

$$\Omega = f_{reso}/f_{c1} = \sqrt{\Omega_s^2 + G/(\pi^2\mu_s\eta)}, \tag{7}$$

where G has two different values as shown in equation (6). It may be said from equation (7) that $\Omega = 1$ means that f_{reso} is tuned to f_{c1}; i.e., $f_{reso} = f_{c1}$.

On the other hand, the frequency equation of the air-gap system with a single gap can be obtained from equation (1) by letting $\bar{X}_1$ be equal to zero. Then, equation (5) leads to $T\bar{X}_2 - 1 = 0$, which can be, by replacing $\bar{X}_2$ with $\bar{X}_s$ for an analogy to equation (7), written as

$$T\bar{X}_s - 1 = 0, \tag{8}$$

where the long-wavelength limit, $T = \tan \pi\Omega\eta \approx \pi\Omega\eta$, has been applied. Finally, one obtains the resonant frequency of the single-gap system from equation (8):

$$\Omega = f_{reso}/f_c = \sqrt{\Omega_s^2 + 1/(\pi^2\mu_s\eta)}. \tag{9}$$

It may be seen from the comparison of equation (9) with equation (7) that the two equations are identical if $G = 1$ in equation (7). Thus, a common resonant frequency equation for both the single-gap and double-gap systems is given by

$$\Omega = \sqrt{\Omega_s^2 + \bar{G}/(\pi^2\mu_s\eta)}, \tag{10}$$

where $\bar{G} = 1$ for the single-gap system and $\bar{G} = G$ for the double-gap system.

2.2. VERIFICATION AND DISCUSSION

To show the validity and accuracy of the closed-form resonant frequency equation, equation (10), approximate resonance frequencies obtained from equation (10) are compared with exact ones obtained by means of plotting equations (2,8), which yield the exact resonant frequencies for the single-gap and double-gap systems respectively. It may be seen in Table 1 that the approximate values agree well with the exact values. In Table 1, Ω_s and μ_s are, respectively, assumed as 0·5 and 2·0, which are reasonable values because they are based on real dimensions and real material properties considered in the next section for experimental verification.

In equation (10), the dimensionless resonant frequency Ω of the air-gap system is a function of Ω_s, μ_s, η, and γ (note that $\bar{G}$ is a function of γ for the double-gap system). Equation (10) implies that Ω is always larger than Ω_s, and that Ω is proportional to Ω_s but is inversely proportional to μ_s and η. It may be said from this fact that the partition sheet used must be designed to be soft so that its natural frequencies, which is simulated by Ω_s, have small values. By this way, the resonant frequency of the air-gap system can be tuned to a lower value and, as a result, the air-gap system can control the resonance of lower acoustic modes of enclosed cavities.

In Figure 2, equation (10) is plotted as η is increased, when $\Omega_s = 0{\cdot}5$, $\mu_s = 2{\cdot}0$, and $\bar{G} = 1$ for the single-gap system ($\bar{G} = 3 \mp \sqrt{5}$ for the double-gap system with $\gamma = 0{\cdot}5$). It may be seen in the figure that a smaller gap thickness is required for the double-gap system than for the single-gap system, because the single-gap system and the double-gap system need $\eta = 0{\cdot}068$ and $0{\cdot}052$ to satisfy $\Omega = 1$ respectively. It may therefore be said from this

TABLE 1

Accuracy of the approximate resonant frequency equation when $\Omega_s = 0{\cdot}5$ and $\mu_s = 2{\cdot}0$

η	Single-gap system		Double-gap system							
			$\eta_1 = \eta/3$				$\eta_1 = 2\eta/3$			
			First		Second		First		Second	
	App.	Exact	App.	Exact	App.	Exact	App.	Exact	App.	Exact
0·01	2·31	2·30	2·17	2·17	5·12	5·12	1·89	1·89	5·91	5·91
0·03	1·39	1·39	1·32	1·31	2·98	2·98	1·17	1·16	3·44	3·43
0·05	1·12	1·12	1·07	1·06	2·33	2·33	0·96	0·95	2·68	2·67
0·07	0·99	0·98	0·94	0·94	1·99	1·98	0·85	0·85	2·28	2·27
0·09	0·90	0·89	0·86	0·86	1·77	1·76	0·79	0·78	2·03	2·02

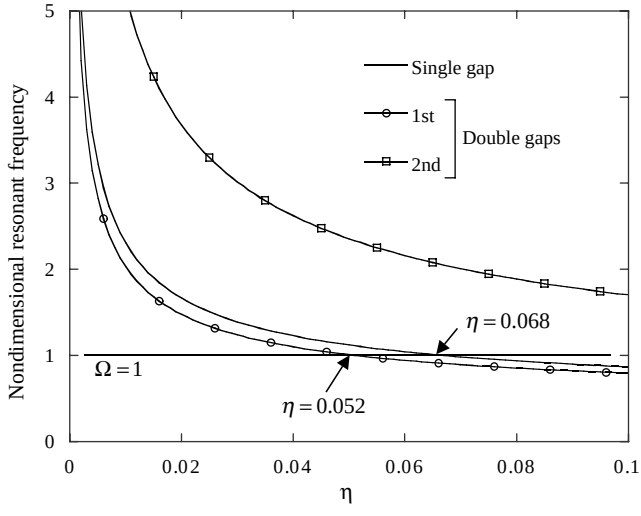

Figure 2. Non-dimensional resonance frequency when $\Omega_s = 0{\cdot}5$ and $\mu_s = 2{\cdot}0$ ($\bar{G} = 1$ for the single-gap system, and $\bar{G} = 3 \pm \sqrt{5}$ for the double-gap system with $\gamma = 0{\cdot}5$).

fact that the double-gap system is more effective than the single-gap system in practical use of space.

On the other hand, $\gamma = \Delta L_1/\Delta L$ involved in $\bar{G}$ influences the resonant frequencies of the double-gap system as confirmed in Figure 3, where the first resonant frequency in the case of $\gamma = 3/4$ requires the smallest value, $\eta = 0{\cdot}041$, to yield $\Omega = 1$. Thus, it is advantageous to design the upper gap thickness ΔL_1 to be larger than the lower gap thickness ΔL_2 when the total gap thickness $\Delta L = \Delta L_1 + \Delta L_2$ is fixed due to the limitation of space. Figure 4 shows the trend of change of the resonant frequencies when γ is changed with $\Omega_s = 0{\cdot}5$ and $\mu_s = 2{\cdot}0$. Here, the first resonant frequency is constantly decreased with increasing γ, but a small amount of decrease is shown, and the second resonant frequency has a minimum value in the vicinity of $\gamma = 0{\cdot}4$ (a large amount of change is shown compared with the first resonant frequency). From this fact, it is concluded that the second resonant frequency can be more effectively tuned to a target frequency than the first resonant frequency, by means of changing the proportion of the upper gap thickness to the lower gap thickness.

3. EXPERIMENT OF THE CAVITY-GAP COUPLING MODEL

Figure 5 shows a box-shaped acoustic cavity manufactured to verify the air-gap effect. When no air gaps or partition sheets are installed, the resonant frequency of the lowest one of the vertical resonant modes, of which pressure variation is formed in the direction of the height of the cavity, can be theoretically calculated to be 184 Hz by $f = c/(2L_z)$. In the paper, the lowest order vertical mode is considered as the target mode that will be controlled by installing the air-gap system as shown in Figure 5. It should be noted that, if an absorbent material sheet is used to suppress the resonance of the vertical mode, its minimum thickness required ought to reach 19 cm corresponding to a quarter of the wavelength of the vertical mode.

As shown in Figure 5, two microphones and a loud speaker for sound generation are put on the bottom of the cavity to measure frequency responses when a partition sheet is set. Two types of partition sheets are used and the first natural frequency and surface

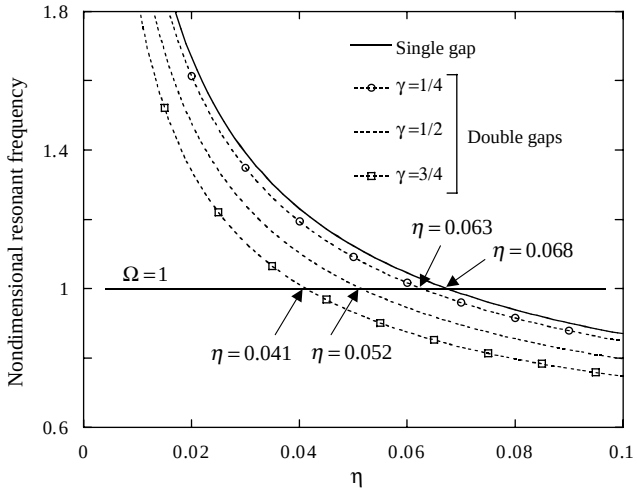

Figure 3. Non-dimensional resonance frequency when $\Omega_s = 0{\cdot}5$ and $\mu_s = 2{\cdot}0$ ($\bar{G} = 1$ for the single-gap system, and $\bar{G}$ is changed for the double-gap system with $\gamma = \frac{1}{4}, \frac{1}{2}$, and $\frac{3}{4}$).

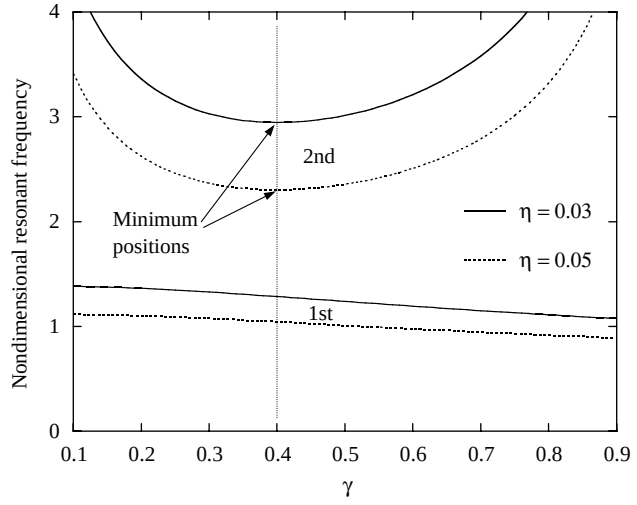

Figure 4. Non-dimensional resonance frequency when γ is changed with $\Omega_s = 0{\cdot}5$, $\mu_s = 2{\cdot}0$ in the case of $\eta = 0{\cdot}03$ and $0{\cdot}05$.

density of each sheet are given in Table 2; the natural frequencies are obtained through vibration modal tests. In addition, the experimental resonant frequencies of the first four vertical modes of the cavity are found to be 173, 358, 556, and 741 Hz without any partition sheet. Particular attention is given to suppressing the first resonance (173 Hz), because a gap of the largest thickness is needed in this case.

3.1. WHEN THE A-PARTITION SHEET IS USED

Figure 6 shows how the acoustic responses vary in the cavity when the gap thickness is increased from 0·0 to 5·5 cm. When the partition sheet is directly attached to the upper

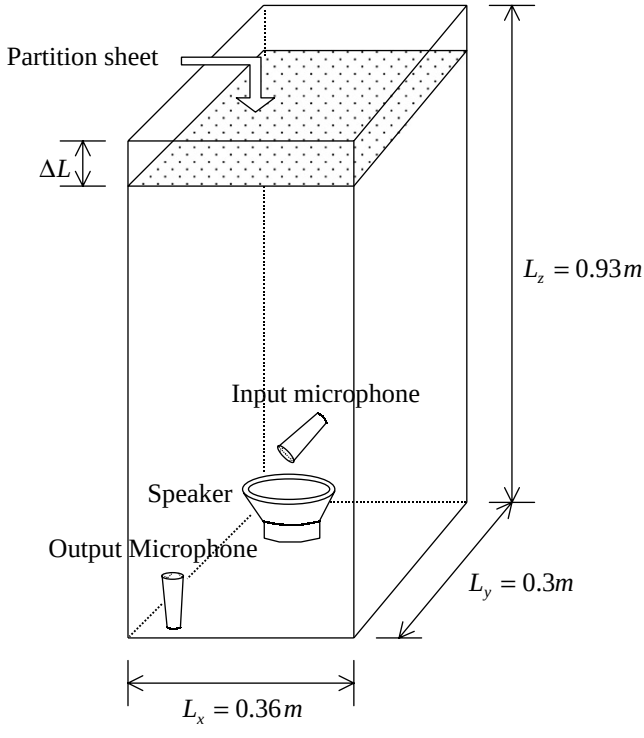

Figure 5. Experimental set-up of a box-shaped cavity for confirming the air-gap effect.

TABLE 2

Surface densities and natural frequencies of the partition sheets used in the experiment.

Partition sheet	Surface density (kg/m^2)	Natural frequency (Hz)			
		First	Second	Third	Fourth
A-type	1·9	72	148	170	240
B-type	2·0	58	128	142	198

boundary of the cavity without any space (see Figure 6(a)), little change appears in the frequency range, 50–850 Hz; the higher resonant peaks above 700 Hz are influenced just a little. When the thickness is increased by 0·5 cm (see Figure 6(b)), it may be seen that the third and fourth peaks, 556 and 741 Hz, drop greatly. As the gap thickness is increased from 1·0 to 6·0 cm, the effect of the air-gap shifts to the lower frequency range. When a value of 3·0 cm is given for the gap thickness (see Figure 6(c)), the second resonant peak (358 Hz) is split into two peaks with almost equal levels. From this fact, the thickness of 3·0 cm may be called a *reasonable gap thickness* for suppressing the second resonant peak. It may also be said from Figure 6(d) that the gap thickness of 5·5 cm is a reasonable gap thickness for suppressing the first resonant peak.

On the other hand, the reasonable gap thickness against the first resonance of the cavity in the experiment can be approximately predicted using equation (10). Ω_s is given by dividing the first natural frequency of the partition sheet by that of the cavity: i.e., $\Omega_s = 72/173\,Hz = 0{\cdot}416$. In addition, μ_s is given by dividing the surface density of the partition sheet by $\rho_{air}L_z$: i.e., $\mu_s = 1{\cdot}9/(1{\cdot}21 \times 0{\cdot}93) = 1{\cdot}688$. In the case of predicting the reasonable

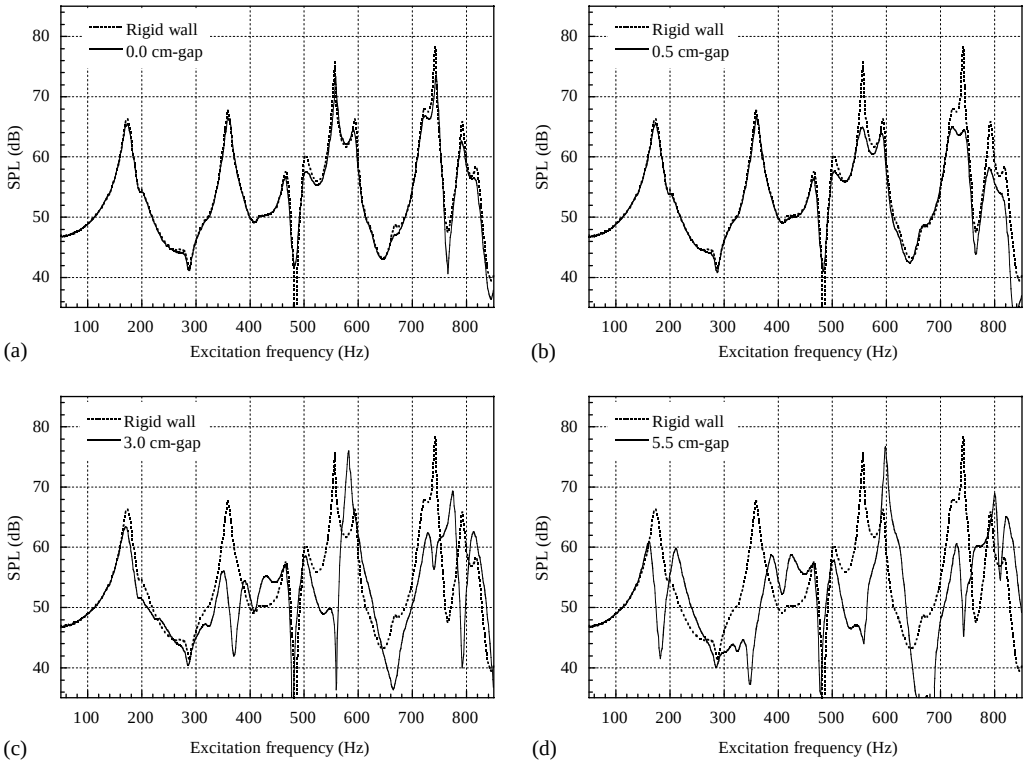

Figure 6. Acoustic responses as the gap thickness is increased with the A-partition sheet: (a) 0·0 cm gap, (b) 0·5 cm gap, (c) 3·0 cm gap, (d) 5·5 cm gap.

gap thickness for the first resonance, Ω is replaced by the unit value ($\Omega = 1$) in equation (10), because Ω approaches the unit value when the resonant frequency of the air-gap system is tuned to the first resonant frequency of the cavity. If $\Omega = 1$, $\Omega_s = 0{\cdot}42$, and $\mu_s = 1{\cdot}69$ are substituted into the corresponding parameters in equation (10), the gap ratio for the first resonance of the cavity is obtained as $\eta = 0{\cdot}073$, which can be translated to $\Delta L = 6{\cdot}79$ cm by multiplying η by L_z. The predicted gap thickness shows a small difference compared with the experimental gap thickness, 5·5 cm. This results from the approximation of the three-dimensional experimental model to the one-dimensional model. It may, however, be said that equation (10) can be used as an important guide in designing the air-gap system.

3.2. WHEN THE B-PARTITION SHEET IS USED

Figure 7 shows the acoustic responses when gaps of 0·0, 0·5, 2·0, and 4·5 cm are used. The acoustic response when no gap is given (see Figure 7(a)) remains almost unchanged compared with the acoustic response when no partition sheet is used. However, when a very small gap of 0·5 cm is given as shown in Figure 7(b), the third and fourth peaks are largely suppressed. This fact suggests that the current thickness, 0·5 cm, is a reasonable thickness only for the third and fourth peaks. The second peak is completely suppressed when the gap thickness is increased to 2·0 cm (see Figure 7(c)), which states that a value of the reasonable thickness for the second peak is 2·0 cm. It may be said from Figure 7(d) that

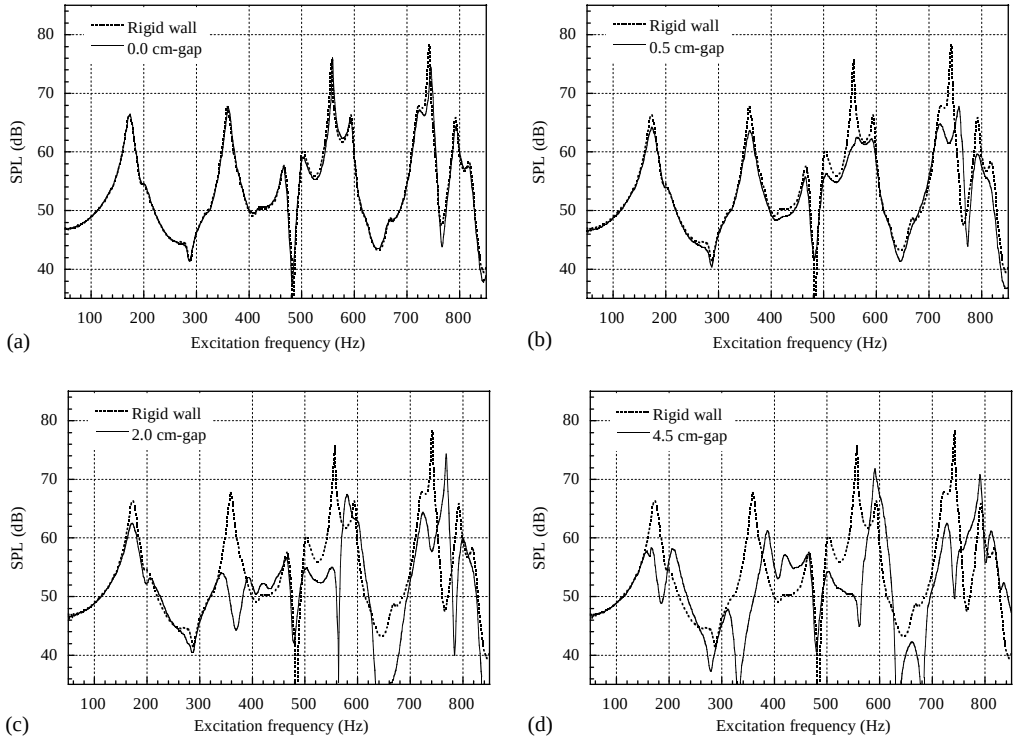

Figure 7. Acoustic responses as the gap thickness is increased with the B-partition sheet: (a) 0·0 cm gap, (b) 0·5 cm gap, (c) 2·0 cm gap, (d) 4·5 cm gap.

the reasonable gap thickness for the first peak is 4·5 cm. It should be noticed that this thickness is 1·5 cm lesser than the reasonable gap thickness for the first peak required when the A-partition sheet is used. In short, the B-partition sheet shows excellent performance than the A-partition sheet, because the first resonant peak can be suppressed with a smaller value when the B-partition sheet is used. The performance of the air-gap system is associated with the first natural frequency and surface density of the partition sheet used. It is noted in Table 2 that the first natural frequency of the B-partition sheet is considerably lower than that of the A-partition sheet.

In the same manner as in section 3.1, a reasonable gap thickness against the first resonance can be predicted using equation (10). In the case of the current partition sheet, Ω_s and μ_s are respectively calculated as $\Omega_s = 58/173\,\text{Hz} = 0{\cdot}34$ and $\mu_s = 2{\cdot}0/(1{\cdot}21 \times 0{\cdot}93) = 1{\cdot}78$ from Table 2. Then, a reasonable gap ratio may be calculated as $\eta = 0{\cdot}064$, which is translated to $\Delta L = 5{\cdot}95\,\text{cm}$, which is somewhat different from the experimental gap thickness, 4·5 cm. It may, however, be said that equation (10) gives reasonable information in designing the gap and the partition sheet, because the predicted gap thickness for the A-partition sheet (5·95 cm) is lesser than that for the B-partition sheet (6·79 cm) in the same manner as in the experiment.

4. CONCLUSION

The air-gap system introduced in the paper can be considered as a sound absorber with effective performance in suppressing low-frequency acoustic resonance in an enclosed

cavity. The closed-form frequency equation, equation (10), can be used as an effectual means in designing the air-gap system for suppressing a target acoustic resonance. In addition, it is shown from the experiments that the modal characteristics of the partition sheets used play an important part in determining the high performance of the air-gap system.

ACKNOWLEDGMENTS

This research was financially supported by Hansung University in the year of 2002.

REFERENCES

1. U. Ingard 1953 *Journal of the Acoustical Society of America* **25**, 1037–1061. On the theory and design of acoustic resonators.
2. M. Alster 1972 *Journal of Sound and Vibration* **24**, 63–85. Improved calculation of resonant frequencies of Helmholtz resonators.
3. R. C. Chanaud 1994 *Journal of Sound and Vibration* **178**, 337–348. Effects of geometry on the resonance frequency of Helmholtz resonators.
4. R. C. Chanaud 1997 *Journal of Sound and Vibration* **204**, 829–834. Effects of geometry on the resonance frequency of Helmholtz resonators, Part II.
5. A. Selamet, P. M. Radavich, N. S. Dickey and J. M. Novak 1997 *Journal of the Acoustical Society of America* **101**, 41–51. Circular concentric Helmholtz resonators.
6. A. Selamet and J. L. Ji 1997 *Journal of the Acoustical Society of America* **107**, 2360–2369. Circular asymmetric Helmholtz resonators.
7. N. S. Dickey and A. Selamet 1996 *Journal of Sound and Vibration* **195**, 512–517. Helmholtz resonators: one-dimensional limit for small cavity length-to-diameter ratios.
8. A. Doria 2000 *Journal of Sound and Vibration* **232**, 823–833. A simple method for the analysis of deep cavity and long neck acoustic resonators.
9. D. Reynolds 1981 *Engineering Principles of Acoustics Noise and Vibration Control*, 333–344. Boston: Allyn and Bacon.
10. L. E. Kinsler 1982 *Fundamentals of Acoustics*, third edition. 225. New York: John Wiley.